Received: 30 March 2024 | Revised: 7 June 2024 | Accepted: 11 June 2024

DOI: 10.1002/pro.5092

RESEARCH ARTICLE

Characterization of βB2-crystallin tryptophan mutants reveals two different folding states in solution

Jiayue Sun[1] | **Ken Morishima**[2] | **Rintaro Inoue**[2] | **Masaaki Sugiyama**[2] | **Takumi Takata**[2]

[1]Department of Chemistry, Graduate School of Science, Kyoto University, Kyoto, Japan

[2]Institute for Integrated Radiation and Nuclear Science, Kyoto University, Osaka, Japan

Correspondence
Takumi Takata, Institute for Integrated Radiation and Nuclear Science, Kyoto University, Kumatori-cho, Sennan-gun, Osaka 590-0494, Japan.
Email: takumi@rri.kyoto-u.ac.jp

Funding information
Japan Society for the Promotion of Science, Grant/Award Number: 23K10868; Japan Science and Technology Agency, Grant/Award Numbers: JPMJFR2007, JPMJFS2123

Review Editor: Aitziber L. Cortajarena

Abstract

Conserved tryptophan residues are critical for the structure and the stability of β/γ-crystallin in the lenses of vertebrates. During aging, in which the lenses are continuously exposed to ultraviolet irradiation and other environmental stresses, oxidation of tryptophan residues in β/γ-crystallin is triggered and impacts the lens proteins to varying degrees. Kynurenine derivatives, formed by oxidation of tryptophan, accumulate, resulting in destabilization and insolubilization of β/γ-crystallin, which correlates with age-related cataract formation. To understand the contribution of tryptophan modification on the structure and stability of human βB2-crystallin, five tryptophan residues were mutated to phenylalanine considering its similarity in structure and hydrophilicity to kynurenine. Among all mutants, W59F and W151F altered the stability and homo-oligomerization of βB2-crystallin—W59F promoted tetramerization whereas W151F blocked oligomerization. Most W59F dimers transformed into tetramer in a month, and the separated dimer and tetramer of W59F demonstrated different structures and hydrophobicity, implying that the biochemical properties of βB2-crystallin vary over time. By using SAXS, we found that the dimer of βB2-crystallin in solution resembled the lattice βB1-crystallin dimer (face-en-face), whereas the tetramer of βB2-crystallin in solution resembled its lattice tetramer (domain-swapped). Our results suggest that homo-oligomerization of βB2-crystallin includes potential inter-subunit reactions, such as dissociation, unfolding, and re-formation of the dimers into a tetramer in solution. The W>F mutants are useful in studying different folding states of βB2-crystallin in lens.

KEYWORDS

cataract, crystallin, inter-subunit interaction, oxidation, SAXS

1 | INTRODUCTION

Native state and correct folding are critical for a protein to function actively. Incorrect folding of proteins or their denaturation after folding due to genetic mutations or amino acid modifications leads to many protein-misfolding diseases, such as Alzheimer's disease, Huntington's disease, Parkinson's disease, and cataract (Chaudhuri and Paul, 2006). Cataract is the leading cause of blindness (Sakthivel et al., 2010) that affects billions of people worldwide. Pathologically, cataract is characterized by the formation of high-molecular-weight insoluble matters from misfolding and aggregation of lens proteins, which scatter the light entering eyes, causing vision loss (Benedek, 1997; Chiti and Dobson, 2006; Feng et al., 2000; Lampi et al., 1998; Moreau and King, 2012; Pande et al., 2001). Understanding the folding pathways of lens proteins is key to comprehending the process of onset of cataracts.

Age-related cataract is associated with aging effects, including continuous eye damage by exposure to ultraviolet (UV) radiation, diabetes, or some acquired eye diseases (Ciechanover and Kwon, 2015; Harding and Dilley, 1976; Robman and Taylor, 2005; Truscott, 2005; Yao et al., 2011). Aging and continuous UV irradiation oxidize tryptophan (Trp; W) in lens proteins to more hydrophilic kynurenine (Kyn) derivatives (Chen et al., 2006; Chen et al., 2009). Lens fiber cells do not have turnover function (Wride, 2011). As the oxidation of Trp increases with age, the native folding states of lens proteins may be disturbed and their stability and solubility is compromised, leading to the onset of age-related cataracts. α-, β-, and γ-crystallins are the three types of lens proteins, comprising 90% of the total proteins in the lens of vertebrates. The three types of crystallin collaborate to maintain the structure and solubility of lens. Although the β/γ-crystallin family members have highly similar primary sequence and tertiary structure (Andley, 2007; Bloemendal et al., 2004; Sliney, 2002), γ-crystallin only exists in monomeric form, whereas β-crystallin can form homo-/hetero-multimeric forms (dimer to octamer) (Bax et al., 1990; Bloemendal et al., 2004; Slingsby and Wistow, 2014). The monomeric states of β- and γ-crystallin possess two domains, connected in the middle via a short peptide (Flaugh et al., 2005). These two domains are pseudo-symmetrical, with each domain containing two Greek key motifs that form a hydrophobic core (Das et al., 2010; Vendra et al., 2013; Xi et al., 2017). Point mutations and post-translational modifications of amino acids including Trp on the Greek key motifs impact the stability and structure of β- and γ-crystallin to varying degrees (Das et al., 2011; Flaugh et al., 2005; Fu and Liang, 2002; Gillespie et al., 2014; Mahler et al., 2011; Mills et al., 2007; Moreau and King, 2009; Sagar and Wistow, 2022; Shiels and Hejtmancik, 2017; Wenk et al., 2000; Zhang et al., 2014). The oxidation effect of Trp has been extensively studied for γ-crystallin (Hains and Truscott, 2008; Schafheimer and King, 2013; Serebryany and King, 2015; Serebryany et al., 2016); however, how oxidation of Trp affects βB2-crystallin remains elusive.

βB2-crystallin is a Trp-rich protein, which contains five Trp residues—W59, W82, W85, W151, and W196 (Figure S1). Except for W196, the other four Trp residues are located in the Greek key motifs of βB2-crystallin. Three Trp-related point mutations, W59C, W151C, and W151R, were reported to be present in βB2-crystallin from patients with various cataracts in China and India (Chaudhuri and Paul, 2006; Xu et al., 2021; Zhao et al., 2017). These findings highlight the significance of Trp residues in the maintenance of the native state of βB2-crystallin. Point mutations are rare findings in age-related cataractous lenses (Bloemendal et al., 2004; Truscott, 2005). Other factors, such as posttranslational modifications including oxidation, may be responsible for cataract formation. Replacing Trp with its oxidized derivatives is technically difficult; therefore, phenylalanine (Phe; F) was used as a substitute. Kynurenine retains the aromatic phenyl ring, but loses the indole ring originated from Trp. At this point, Phe has structural similarity with kynurenine, especially with regard to the presence of the phenyl ring. Therefore, we used W>F as an "early stage oxidation model" for studying the Trp oxidation pathway.

For the oligomeric states of βB2-crystallin, there is a discrepancy between dimers formed in crystal and in solution. The lattice dimer, which consists of two monomers with opposite domain alignment (domain-swapped, Figure S2), is derived from the tetrameric crystal structure (7K7U.pdb) of βB2-crystallin (Smith et al., 2007; Van Montfort et al., 2003). The in-solution dimer was found to resemble truncated βB1-crystallin dimer (1OKI.pdb), which consists of two monomers with domains facing each other (face-en-face, Figure S2) (Xi et al., 2017). The first published crystal structure of βB2-crystallin was a tetramer with two domain-swapped dimers, and thereafter, the domain-swapped dimer was considered a key characteristic of βB2-crystallin (Bax et al., 1990). However, the βB2-crystallin dimer in solution has the shape of domain-swapped dimer, but acquires a more compact structure named face-en-face (Xi et al., 2017). These findings raised the question as to whether βB2-crystallin folds differently in solution and in the crystal form. Because βB2-crystallin forms not only dimers in solution in vivo and in vitro, we questioned as to how other oligomeric states of βB2-crystallin fold in solution. In this study, we

mutated the five βB2-crystallin Trp residues to Phe to investigate the contribution of each Trp to the folding states and stability of βB2-crystallin. We employed small angle x-ray scattering (SAXS) experiments to structurally analyze the different oligomeric states of βB2-crystallin homomers. This study provides insights into the effect of Trp oxidation on the biochemical properties of βB2-crystallin and the results shed light on understanding βB2 aggregation and age-related cataract formation.

2 | RESULTS

2.1 | Effects of Trp oxidation on the stability and structure of βB2-crystallin

Each Trp residue in the human βB2-crystallin sequence was replaced with Phe to study the effect of Trp oxidation on the structure and stability of βB2-crystallin (Figure S1). During purification of the mutated proteins, white precipitates appeared for W59F, but not for the other mutants, which implied that W>F mutants of βB2-crystallin lowered its stress resistance. Therefore, the thermal stability of each βB2-crystallin mutant was measured by determining the index of precipitation with increasing temperature. The recombinant wild type (WT) protein was more heat stable than the mutants in that it formed white precipitates at 68°C, whereas W82F, W85F, W151F, and W196F formed precipitates at approximately 65°C (Table 1 and Figure S3), indicating a slight decrease in heat stability caused by these four mutations. Notably, the temperature for precipitation of W59F was approximately 56°C, implying that W59F was much less heat stable than the WT and other mutants.

Because four of the five Trp residues in βB2-crystallin are located on the β-sheets of the Greek key motifs, we used far-UV circular dichroism (CD) to analyze the conformational changes in the secondary structure among βB2-crystallin mutants. The secondary structures of all the βB2-crystallin mutants were highly similar to that of the WT (Figure 1). However, W59F showed a left-shift pattern with a sharp signal near 203 nm (Figure 1a), indicating a slightly disordered Greek key motif in the N-terminal domain of βB2-crystallin whereas other spectra exhibited identical peaks between 205 and 217 nm (Figure 1b–e).

Intrinsic Trp fluorescence provides clues on the regional structure around a Trp residue in proteins (Kosinski-Collins and King, 2003; Kosinski-Collins et al., 2004). To examine the location effect of each Trp residue on βB2-crystallin, the intrinsic Trp fluorescence for each W>F mutant was measured (Figure 2). The fluorescence intensity of the βB2-crystallin mutants was in the order W196F > W82F > W85F > W151 ≈ W59F. W59F and W151F exhibited the lowest intrinsic fluorescence intensity with a right-shift compared with the spectrum for the WT, indicating partially disordered tertiary structures (Figure 2b). The intrinsic fluorescence intensity for W82F, W85F, and W196F was lower than that for WT because these mutants contain one less Trp than the WT, but no right-shift was noted for the mutants, which indicates that they were in a similar folding state as WT.

The Greek key motifs of βB2-crystallin form the hydrophobic core, and disordering of these motifs disturbs the compactness of the core and alters the extent of hydrophobic areas exposed. To determine whether partially denatured W59F and W151F βB2-crystallin mutants had altered hydrophobicity, we performed the bis-ANS binding assay (Figure 3). Bis-ANS is a non-covalent extrinsic fluorescent dye that interacts with the hydrophobic regions on the target protein through its phenyl and naphthyl rings. The WT and W151F proteins exhibited almost the same bis-ANS fluorescent intensity, whereas W59F showed a much more intense bis-ANS fluorescent peak indicating that the hydrophobic region in W59F was much more exposed than in W151F and in WT (Figure 3).

TABLE 1 Turbidity measurement of βB2 WT and its mutants.

βB2 sample	Temperature of turbidity initiation (°C)	Temperature error (°C)
WT	64.7	±0.01
W59F	54.4	±0.08
W82F	66.4	±0.69
W85F	62.5	±0.06
W151F	63.2	±0.03
W196F	65.1	±0.01

Note: All mutations lowered the temperature of turbidity initiation. W59F decreased the heat stability of βB2.
Abbreviation: WT, wild type.

2.2 | Oxidation affects homo-oligomerization of βB2-crystallin

βB2-crystallin exists as both homo- and hetero-oligomer in lens. Many studies have shown that βB2-crystallin is mainly dimeric in solution but can also form higher-order homomers (Bloemendal et al., 2004; Xi et al., 2017; Zhao et al., 2017). To observe the effect of oxidation on the oligomeric state of βB2-crystallin, we performed analytical size exclusion chromatography (SEC) experiments using fresh βB2-crystallin mutants (Figure 4). All mutants, except for W151F, showed a huge peak for

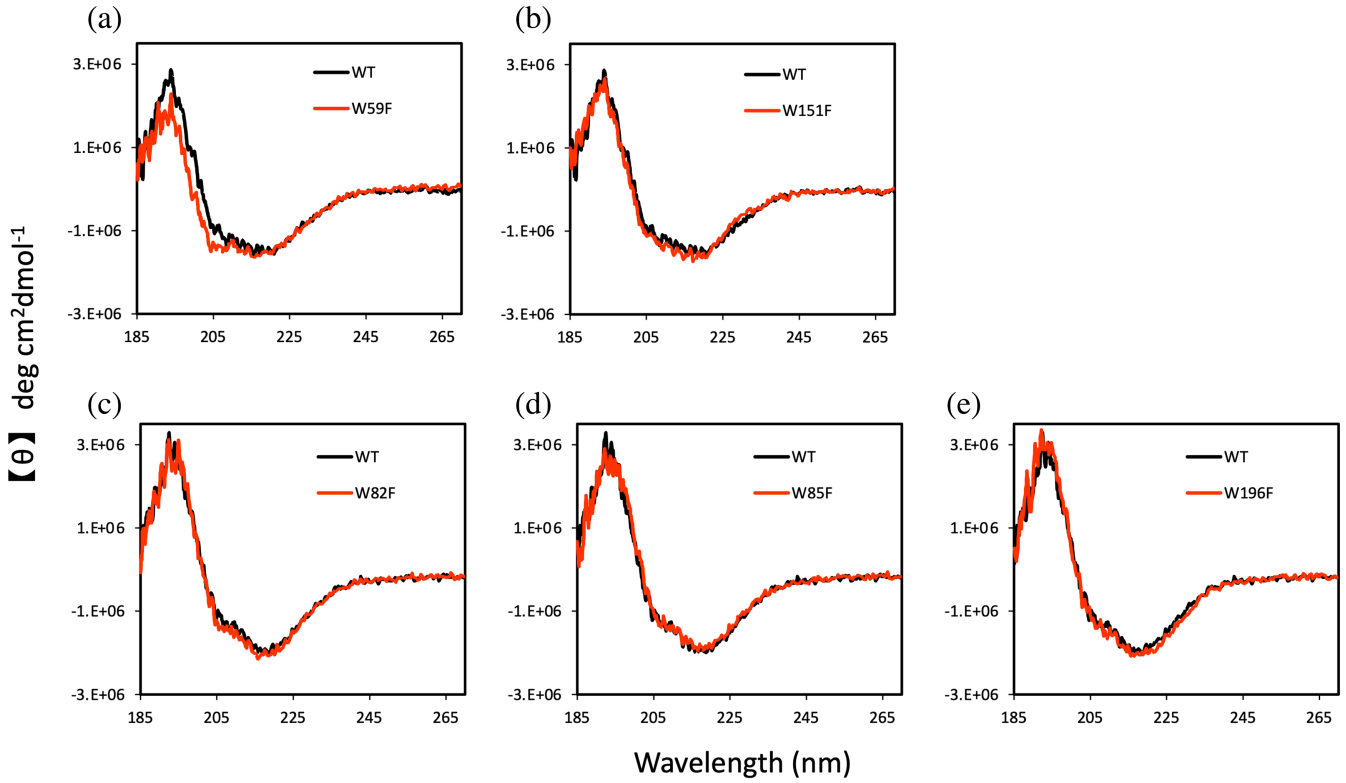

FIGURE 1 Comparison of βB2 secondary structures among mutants. WT is shown in black, and the mutants are shown in red. (a) W59F has a left-shift on its CD pattern indicating potential disorders on the Greek key Motifs. (b–e) W151F, W82F, W85F, and W196F bear no differences in secondary structure compared to WT. CD, circular dichroism; WT, wild type.

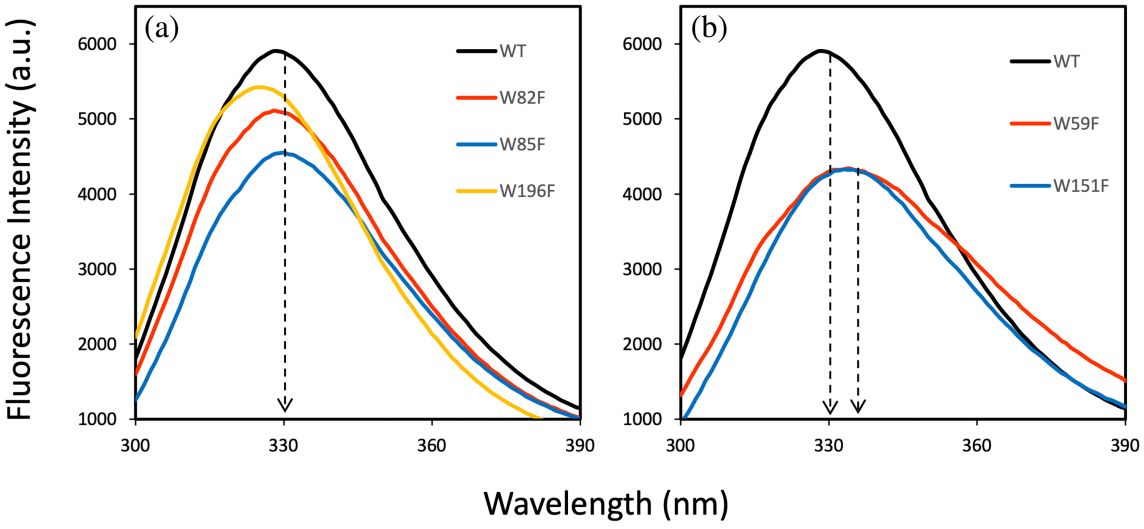

FIGURE 2 Intrinsic Trp fluorescence of βB2 WT and its mutants. (a) WT is shown in black; W82F is shown in red; W85F is shown in blue; W196F is shown in yellow. (b) WT is shown in black; W59F is shown in red; W151F is shown in blue. W151F and W59F have the lowest Trp fluorescence intensities, and they exhibit a right-shift pattern, indicating partial unfolding of the βB2 structure. WT, wild type.

dimer and a small peak for tetramer; W151F only showed a peak for dimer. Comparison of the peak area of the tetramer and dimer for each sample showed that W59F formed more tetramers than the other samples (Figure 4a). Shoulder peaks in the W59F chromatogram were indicative of multiple oligomeric states. Moreover, an equilibrium was noted between dimer and lower-order oligomers, and between tetramer and higher-order oligomers for W59F (Figure 4a). To quantify each oligomeric state for the βB2-crystallin mutants, we performed

analytical ultra-centrifugation (AUC) (Table 2). Dimer is the main oligomeric state for all βB2-crystallin mutants in solution, whereas tetramer is the second most predominant oligomeric state. Surprisingly, except for WT, the monomer content for all the other mutants was small. Among all mutants, tetramer (36.1%) and monomer (15.3%) were the most predominant states for W59F, whereas almost no tetramer (2.7%) was formed by W151F. The AUC results verified our SEC data. W85F had smaller amounts of the tetramer than the other mimics (Figure 4), but the AUC results suggested the presence of the tetramer as in the other mimics. Therefore, we surmised that W151F is the only mutant that does not form tetramers.

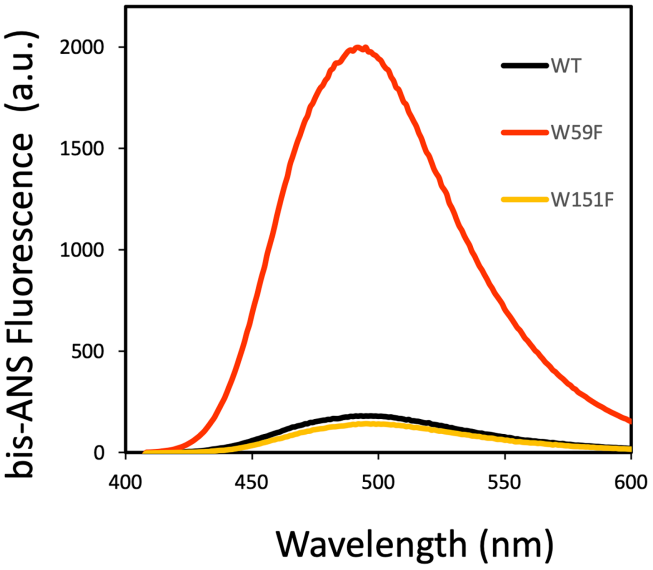

FIGURE 3 Bis-ANS measurements of βB2-WT, W59F, and W151F. WT is shown in black; W59F is shown in red; W151F is shown in yellow. W59F is more hydrophobic than WT and W151F. WT, wild type.

Because time may also alter the oligomeric state of βB2-crystallin, we again performed SEC for W59F, the most unstable among all the mutants, after a month (Figure S4). Notably, more W59F tetramers were found than dimers, indicating that the equilibrium shifted toward the higher-order oligomeric state. To differentiate between these two states of W59F, we extracted the dimers and tetramers and performed extrinsic bis-ANS and intrinsic Trp fluorescence examinations (Figure 5). The dimer was more hydrophobic than the tetramer (Figure 5a), whereas the dimer exhibited lower Trp fluorescence and a right-shift than the tetramer (Figure 5b). Our results suggested structural differences between dimer and tetramer; the

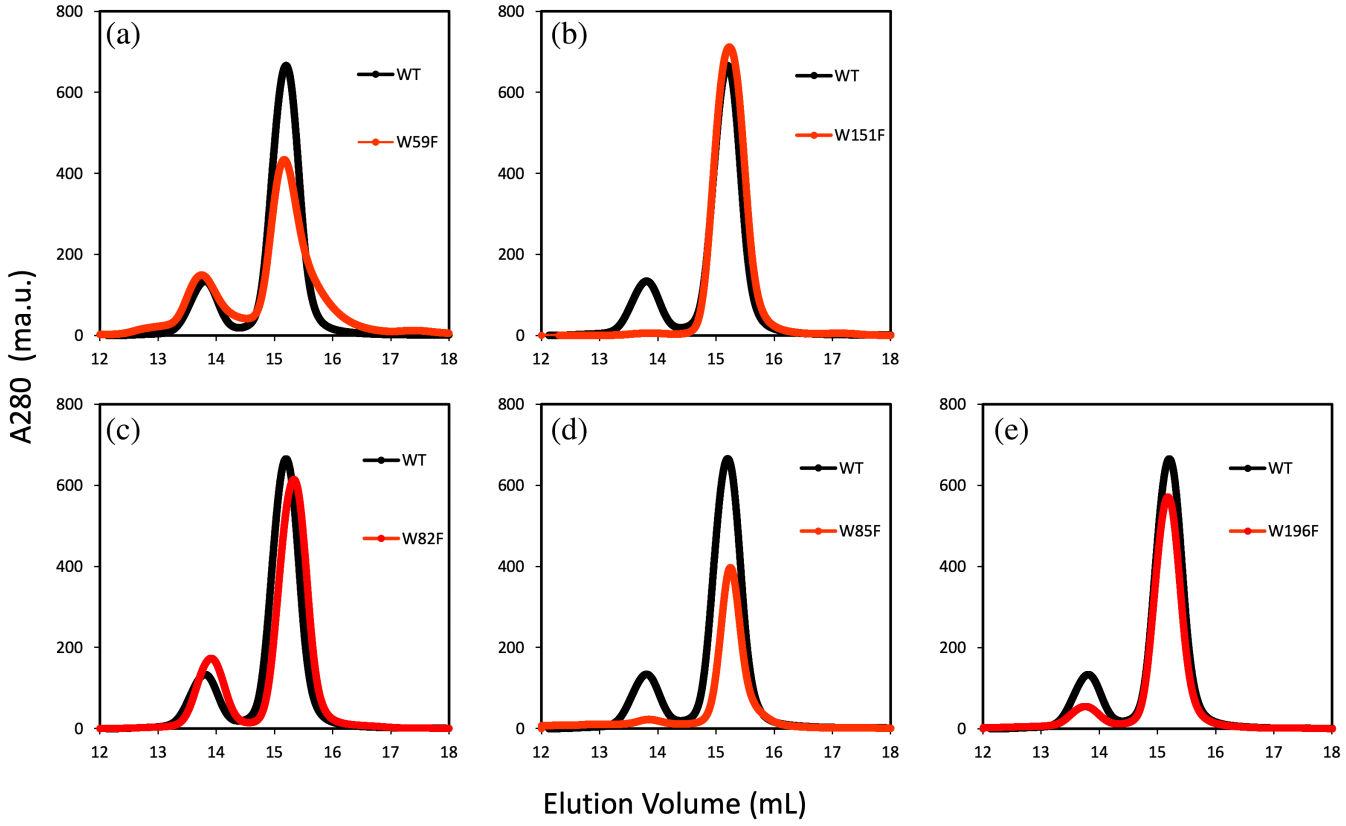

FIGURE 4 Size comparison between βB2-WT and its mutants using SEC. WT is shown in black; its mutants are shown in red. (a, c, d, and e) W59F, W82F, W85F, and W196 all show equilibrium between their dimer and tetramer forms. (b) W151F only demonstrates a dimeric peak. SEC, size exclusion chromatography; WT, wild type.

hydrophobic regions evident in the dimer might be buried in the tetramer.

The biochemical differences between homo-oligomeric states of βB2-crystallin prompted us to question the process of oligomerization of βB2-crystallin dimers into tetramers. To decipher the folding states of βB2-crystallin, we employed SAXS equipped with SEC (SEC-SAXS) for W59F (dimers and tetramers were extracted separately), WT, and W151F. The results indicated that mostly WT was still in its dimeric form and W151F did not form more higher-order oligomers during 1 month of storage unlike W59F (Figure S5).

2.3 | SAXS-based structural characterization of βB2-crystallin folding states

According to the lattice domain-swapped dimeric structure of βB2-crystallin, W59 and W151 are almost in superimposition, which indicates that W59F and W151F shall share a similar pattern of homo-oligomerization that is not consistent with our results. Therefore, in-solution structures of βB2-crystallin mutants were investigated using a series of SEC-SAXS experiments (Figures 6–8). SEC was performed to ensure the monodispersity of samples. AUC was applied to W59F tetramer after SAXS (AUC-SEC) to eliminate the aggregation effect. The results indicated that the scattering profiles of the dimers of W59F and W151F were consistent with that of the WT in size (Figure 6a,b, and Table S1). The calculated radius of gyration (R_g) for the WT, W59F, and W151F dimers was 22.7 ± 0.3 Å, 23.0 ± 0.7 Å, and 22.6 ± 0.2 Å, respectively, indicating identical size of all the three dimers. The scattering profile of the W59F tetramer was similar to that of WT (Figure 6c and Table S1). The calculated R_g for WT and W59F tetramer was 29.9 ± 1.0 Å and 30.0 ± 0.3 Å, respectively, indicating the identical size of these two tetramers.

Xi et al. (2017) reported that the dimeric structure of βB2-crystallin in solution is face-en-face (Xi et al., 2017), not domain-swapped. The dimeric state of βB2-crystallin in crystal and solution was differentiated; however, in-solution structures of higher-order βB2-crystallin oligomers had never been solved. To clarify the tetrameric state of βB2-crystallin and compare it with its dimeric state, we generated scattering profiles for lattice domain-swapped dimer, lattice tetramer from βB2-crystallin, and lattice face-en-face dimer from βB1-crystallin (Figures 7 and 8). The overall fit of the W151F dimer to the domain-swapped dimer was poor ($\chi^2 = 67.7$); instead, the W151F dimer showed a good-fit to the face-en-face dimer ($\chi^2 = 3.7$) (Figure 7a). The calculated R_g for the W151F dimer was 22.6 ± 0.2 Å, which is consistent with the R_g for the lattice truncated βB1-dimer (22.5 Å), but much different from the R_g of the lattice domain-swapped βB2-dimer (28.2 Å) (Figure S6). Our results were consistent with those of Xi et al. (2017).

TABLE 2 AUC generated oligomeric states of βB2 WT and its mutants.

Sample	% monomer	% dimer	% tetramer
WT	0	91.7 ± 0.7	8.3 ± 0.1
W59F	15.3 ± 0.3	48.7 ± 0.3	36.1 ± 0.4
W82F	2.3 ± 0.1	75.5 ± 0.3	22.3 ± 0.2
W85F	8.7 ± 0.1	79.7 ± 0.6	11.5 ± 0.6
W151F	5.1 ± 0.1	92.2 ± 0.5	2.7 ± 0.1
W196F	3.8 ± 0.1	83.4 ± 0.4	12.7 ± 0.4

Note: W59F formed more tetramers than the other samples.
Abbreviations: AUC, analytical ultra-centrifugation; WT, wild type.

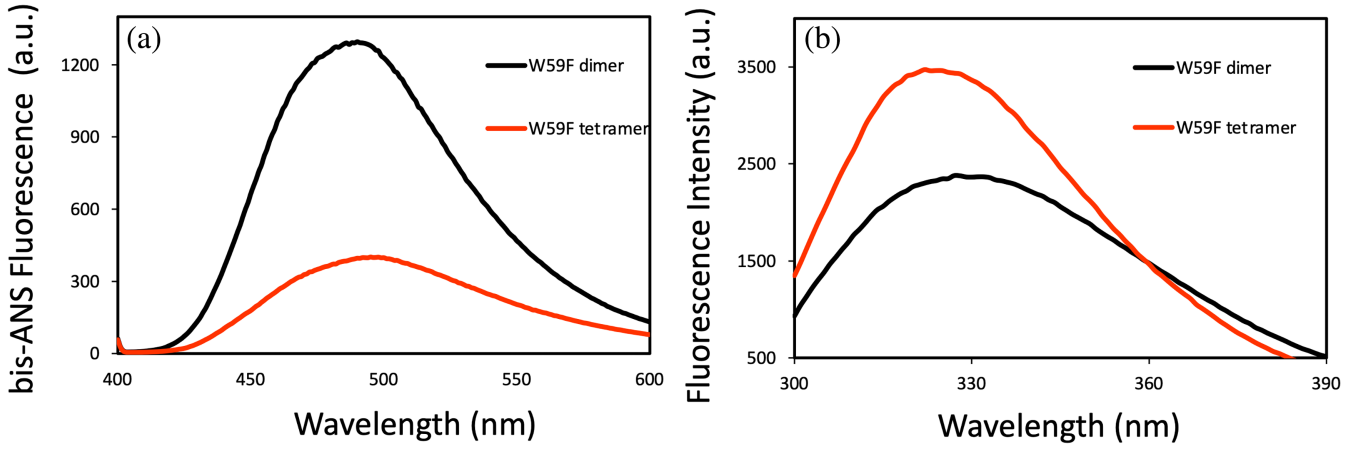

FIGURE 5 Fluorescence measurements of the extracted W59F dimer (black) and tetramer (red). (a) Extrinsic bis-ANS fluorescence shows that the tetramer is less hydrophobic than the dimer. (b) The tetramer has more intense Trp fluorescence than the dimer.

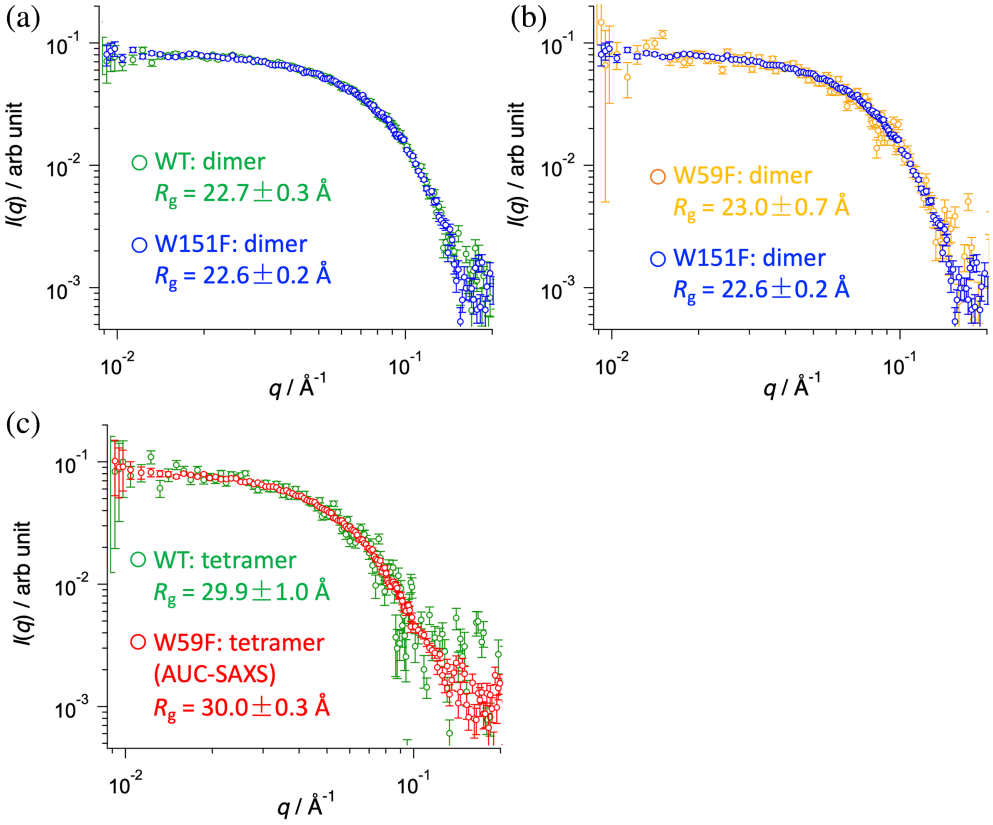

FIGURE 6 Scattering profiles of βB2 dimer and tetramers with calculated R_g. (a and b) The dimers of WT, W59F, and W151F are consistent in size. (c) WT tetramer and W59F tetramer are consistent in size. WT, wild type.

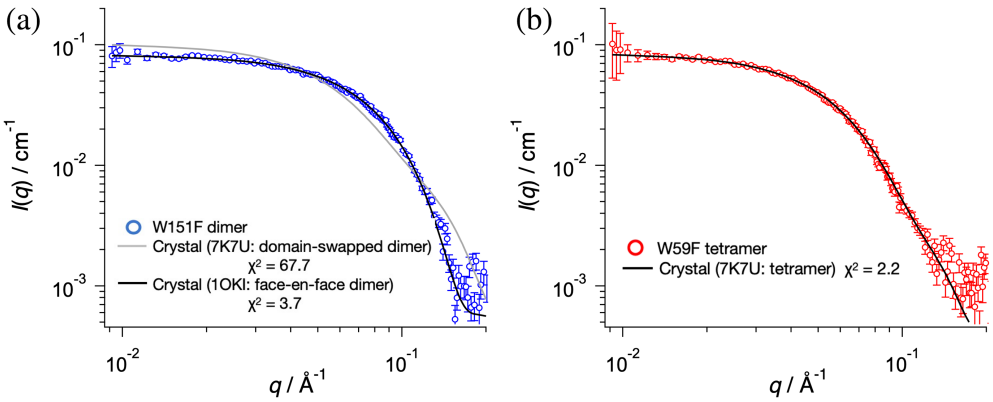

FIGURE 7 Comparison between βB2 samples and their crystal scattering profiles. (a) Scattering profile overlap between W151F dimer, crystal-derived βB2 domain-swapped dimer, and crystal-derived truncated βB1 face-en-face dimer. (b) Scattering profile overlap between W59F tetramer and crystal-derived βB2 domain-swapped tetramer.

Surprisingly, the W59F tetramer was well-fitted to the lattice tetramer that contains two domain-swapped dimers ($\chi^2 = 2.2$) (Figure 7b). The calculated R_g for the W59F tetramer was 30.0 ± 0.3 Å, which is consistent with the R_g for the lattice tetramer (30.1 Å) within the range of experimental error (Figure S7). The superposition of the ab initio model with different lattice structures provided a straightforward comparison between the in-solution and in-crystal folding states of βB2 (Figure 8). The Kratky plots (Figures S6 and S7) of the W59F tetramer and W151F dimer exhibited a bell-shaped distribution, indicating the well-folding status of the samples in solution.

3 | DISCUSSION

3.1 | Oxidation impacts the stability and structure of βB2-crystallin

Five W>F mutants of βB2-crystallin were generated to mimic the oxidative modification at each of the Trp sites in the protein. W59 and W151 are two susceptible residues, the mutations of which greatly impacted the stability and inter-subunit interaction of βB2-crystallin. W59F exhibited a small, disordered structure on the Greek key motif at the N-terminal domain, resulting in more exposure of the hydrophobic surface (Figures 1–3). W59F was

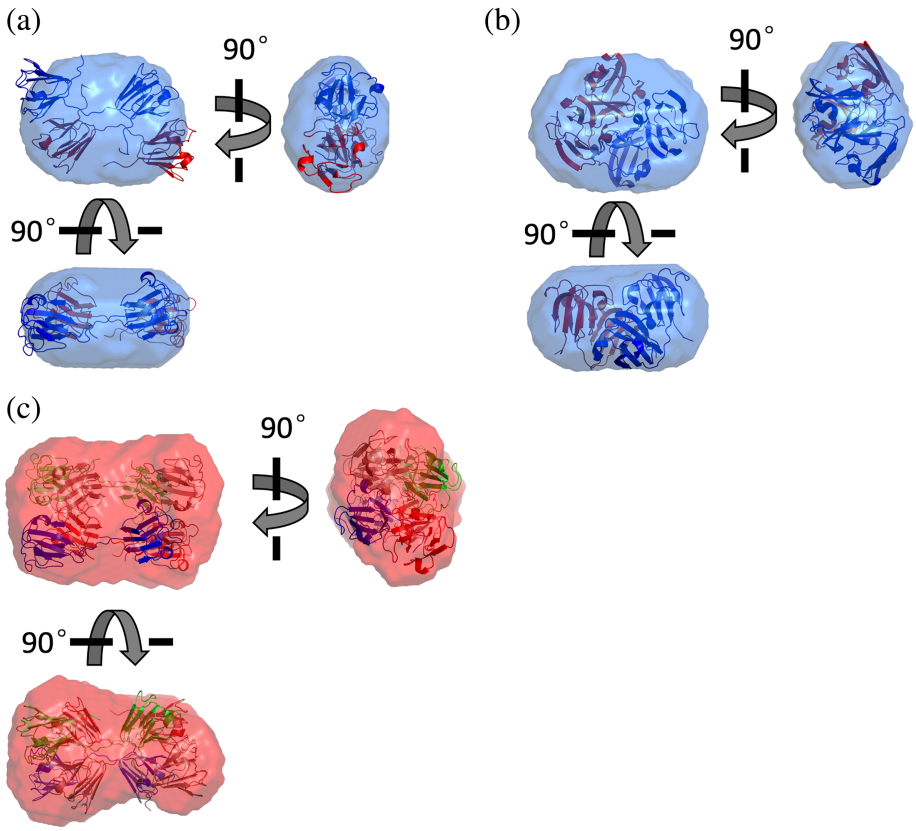

FIGURE 8 Superposition of dimer and tetramer ab initio models with βB2-crystallin crystal structures. (a) Superposition of ab initio model and domain-swapped dimer (extracted from 7K7U.pdb). (b) Superposition of ab initio model and face-en-face dimer (1OKI.pdb). (c) Superposition of ab initio model and crystal lattice tetramer (7K7U.pdb).

relatively unstable under stress such as heat (Table 1) and over time (Figure S4), probably because of the exposed hydrophobic surface, which opened-up the hydrophobic core and allowed the entry of water molecules that disturbed structural stability of βB2-crystallin. Upon further analysis of the W59F dimer and tetramer (Figure 5), these two oligomeric states were found to have different structures, which were confirmed using SEC-SAXS experiments (Figures 6–8). The R_g of the βB2-crystallin dimer is slightly smaller than that of ovalbumin, indicating that the shape of β-crystallin dimer deviated slightly from the spherical shape (Morishima et al., 2023). The different R_g values for the βB2-crystallin tetramer and rabbit enolase, which has a similar molecular weight, implies an aspherical shape of the βB2 tetramer (Smilgies and Folta-Stogniew, 2015). The difference in hydrophobicity between the W59F dimer and tetramer implied that the exposed hydrophobic surfaces in the dimer might participate in the folding process to promote the formation of tetramers.

W151F did not exhibit any secondary structure disorder in CD; however, intrinsic Trp fluorescence suggested that partial misfolding or unfolding happened around W151F (Figures 1 and 2). However, this conformational change did not substantially impact the heat stability (Table 1) or alter the hydrophobicity of βB2-crystallin (Figure 3). In contrast to W59F, W151F blocked the inter-subunit interaction of βB2-crystallin, implying that the oxidation at W151 might prevent homo-oligomerization of βB2-crystallin. From a structural perspective, W59 and W151 are present in the center of the N-/C-terminal domain of monomeric βB2-crystallin and appear on the interface of two monomers to form a dimer. W82 and W85 are present in the relatively peripheral regions, and W196 is located on the C-terminal extension. These three Trp positions are not as structurally important as W59 and W151; thus, W>F mutations at these three positions had less impact on the overall Trp environment in βB2-crystallin.

3.2 | Two in-solution folding states of βB2-crystallin

Under crystallization conditions, proteins are prone to form high-order oligomers, and the lattice dimer of βB2-crystallin is not favored. The current lattice domain-swapped dimer is derived from the real crystal tetramer of human βB2-crystallin (7K7U.pdb), which means that whether this lattice dimeric state exists in the βB2-crystallin folding process remains in question. Our SEC-SAXS results support the face-en-face model (Xi et al., 2017), in which the βB2-crystallin dimer resembles the truncated βB1-crystallin dimer in solution (Figures 6–8, Figures S6 and S7).

In general, the high-order oligomers of a protein are built by its subunits. The high-order oligomeric structures have been used in many studies to predict subunit conformation due to technical problems. In lens, crystallin folding is a multi-step process, and each step can be susceptible to protein misfolding and dysfunction. For this reason, were solved the tetrameric structure of βB2-crystallin and compared it with the dimeric structure in solution using SEC-SAXS. This is the first time that βB2-tetrameric structure in solution has been clarified and, to our surprise, has been found to be consistent with the lattice domain-swapped tetramer.

Our results provide insights that in the process of folding of βB2-crystallin in solution, compact face-en-face dimers need to go through intermediate reactions to form a domain-swapped tetramer. The folding process may include unfolding and/or dissociation of the face-en-face dimeric state into two monomers, which extends the domain-linker peptide on the way, followed by the N-terminus of one monomer swapping with the C-terminus of another monomer to generate the domain-swapped dimers. Our AUC data do show an equilibrium between monomer and dimers of βB2-crystallin mutants (Table 2, Table S2), which supports our speculation regarding the βB2-folding pathway. A similar dissociation and re-formation of dimers has also been suggested for the polymerization scheme of γ-crystallin (Das et al., 2011) and βB2/βA3-crystallin heteromer (Lampi et al., 2016). Additionally, homo-oligomerization takes time; our results implied that different oligomeric states of crystallin formed at different stages of the folding process might possess different biochemical properties (Figure 5) and might have varied functions in lens.

3.3 | Implications of oxidative damage on cataract formation

Many posttranslational modifications in lens crystallin accumulate spontaneously with aging. They induce abnormal inter-subunit interactions within lens proteins to form high-molecular-weight oligomers and/or aggregates. Thus, oligomeric states of crystallin also keep changing over the lifespan. Our results imply that the oxidation of W59 destabilizes βB2-crystallin dramatically and opens homo-polymerization (Table 1 and Figure S4), which is a potential pathway for the formation of βB2-crystallin aggregates to cause age-related cataracts. Previous research has revealed that upon UV-B irradiation, Trp and its nearby cysteine (Cys; C) in human γD-crystallin are oxidized and promote polymerization (Schafheimer and King, 2013). βB2-crystallin has two Cys residues, namely C38 and C66. These two Cys residues are relatively close to W59; therefore, the inter-molecular disulfide bond may be one reason for the promotion of aggregate formation in the W59 mutant. In a non-native octameric structure of γS-crystallin, C24 in one subunit was also found to form a disulfide bond with C24 in another subunit (Sagar and Wistow, 2022). C38 in βB2-crystallin is analogous to C24 in γS-crystallin. We believe that disulfide bonding around W59 is critical for the homo-oligomerization of βB2-crystallin. W151 is also a susceptible position for cataract, considering W151C and W151R are point mutations found in patients with congenital nuclear cataracts and progressive membranous cataracts, respectively (Xu et al., 2021; Zhao et al., 2017). However, the result from W151 mutant was different from those of W59 mutant. W151F prevented homo-oligomerization of βB2-crystallin in vitro. Oxidation at W151 may make some other contributions toward cataract formation in vivo.

Overall, we found that the oxidation of W59 and W151 impacted the structure, stability, and homo-oligomerization of βB2-crystallin. Currently, research on protein folding pathways is limited because different folding intermediates of a protein are difficult to trap, and the folding steps are too fast to analyze. Using our W>F modules, we characterized the tetrameric state of βB2-crystallin in solution for the first time, confirmed the dimeric face-en-face model suggested by the Gronenborn group (Xi et al., 2017), and obtained insights into the βB2-folding pathway that is critical for understanding the onset of age-related cataract.

4 | METHODS

4.1 | Chemicals and materials

MES and EDTA were purchased from DOJINDO (Kumamoto, Japan). Urea was purchased from Sigma-Aldrich (MO, USA). Bis-ANS was purchased from Cayman Chemical (MI, USA). IPTG was purchased from Protein Ark (Sheffield, UK). All other chemicals were obtained from FUJIFILM Wako Pure Chemical Corporations (Osaka, Japan).

4.2 | Plasmids and site-directed mutagenesis

The human CRYBB2 gene was used to generate single-site mutants using the Lightning site-directed mutagenesis kit (Agilent, CA, USA) with primers (Table S3) synthesized by Eurofins Genomics (Tokyo, Japan). The βB2-WT cloned in the pET28a vector with ampicillin resistance gene was used as a template to

proceed with mutagenesis employing the polymerase chain reactions as per the protocol suggested by Agilent. The PCR products were transformed into XL-10 Gold cells, and DNA was extracted from the transformed bacterial cells to obtain recombinant plasmids. The new constructs were verified using DNA sequencing, which was performed by Eurofin Genomics.

4.3 | Protein expression, purification, and characterization

The overexpression of the βB2-crystallin mimics in BL21-pLysS (Thermo Fisher Scientific, MA, USA) was induced with 0.3 mM IPTG at an optical density of 0.5. The cells were cultured for 4 h at 37°C after IPTG induction. The harvested cells were sonicated and resuspended in buffer [20 mM Tris (pH 7.8) 1 mM EDTA, 1 mM DTT], and then loaded onto a Hiprep™ Q XL 16/10 anion exchange column. The target proteins were eluted with the elution buffer [20 mM Tris (pH 7.8), 1 mM EDTA, 1 mM DTT, 1 M NaCl]. The eluted fractions were pooled, buffer-exchanged into a different buffer [20 mM MES (pH 5.8), 1 mM EDTA, 1 mM DTT], and then loaded onto a Hiprep™ SP XL 16/10 cation exchange column. The target proteins were eluted with an elution buffer [20 mM MES (pH 5.8), 1 mM EDTA, 1 mM DTT, 500 mM NaCl]. The purified proteins were buffer-exchanged into SEC buffer [20 mM Tris (pH 7.8), 150 mM NaCl] for SEC, AUC, and SAXS experiments, or into 50 mM phosphate buffer (Na-pi, pH 7.3) for CD, fluorescence, and turbidity measurements. The purity (>95%) of each purified protein was confirmed by electrophoresis on a 12% sodium dodecyl sulfate polyacrylamide gel (SDS-PAGE) under reducing conditions (Figure S8). The concentration of all the proteins was measured at 280 nm.

4.4 | CD spectroscopy

Far-UV CD spectra for βB2-crystallin mimics were measured using a J-805 spectropolarimeter (JASCO, Tokyo, Japan). Each protein sample was prepared at a concentration of 0.2 mg/mL in 50 mM Na-pi buffer (pH 7.3). The measurements were carried out in a 0.02 cm-pathlength cell at 25°C. The buffer blank was subtracted from all spectra.

4.5 | Turbidity measurement

Turbidity was measured over a temperature range from 20 to 90°C using a V-730 spectrophotometer (JASCO), equipped with a water bath to control the temperature and a temperature sensor that could be inserted into the cell. Turbidity, as a function of temperature, was recorded at 450 nm with continuous stirring at 700 rpm for all protein samples at a concentration of 0.4 mg/mL. We used the following equation to reproduce the temperature dependence of mimics.

$$\text{Absorbance} = a + \left(\frac{b}{1+\exp((c-T)/d)}\right), \qquad (1)$$

where a, b, c, and d are the fitting parameters and T is the temperature. A fitting parameter, c, was used as the turbidity temperature.

4.6 | Intrinsic Trp fluorescence assay

The intrinsic Trp fluorescence of βB2-crystallin mimics was measured using an FP-8250 spectrophotometer (JASCO) with a 1 mm-pathlength cell. The intrinsic Trp fluorescence of W59F dimer and tetramer was measured using an F-4500 fluorescence spectrophotometer (HITACHI, Tokyo, Japan) with a 1 mm-pathlength cell. The excitation wavelength was set to 290 nm and the spectra were recorded over a wavelength ranging from 300 to 400 nm for all samples at a concentration of 0.02 mg/mL.

4.7 | Extrinsic bis-ANS binding assay

The extrinsic bis-ANS fluorescence was measured using an FP-4500 spectrophotometer (HITACHI) with a 1.0 mm-pathlength cell. The excitation wavelength was set to 390 nm. bis-ANS (0.01 mg/mL) was mixed with protein sample at a final sample concentration of 0.02 mg/mL. Spectra were recorded over a wavelength ranging from 400 to 600 nm to measure the hydrophobicity exposure of the protein samples.

4.8 | Analytical SEC

All protein samples were concentrated to 4.0 mg/mL in SEC buffer, and then filtered through a 0.45 μm PVDF membrane (Merck Millipore, Co. Cork, Ireland). Each protein sample (500 μL) was injected into the Superdex™ 200 Increase 10/300 column equipped on an AKTA GO purifier system (Cytiva). The flow rate was 0.3 mg/mL, and resultant peaks were compared with the SEC-SAXS and AUC data.

4.9 | AUC

The AUC experiments were performed using ProteomeLab XL-I (Beckman Coulter, USA). The samples were loaded into cells equipped with 12 mm-pathlength aluminium center pieces (Beckman Coulter, USA). The sedimentation-velocity method was employed using Rayleigh interference optics at a rotor speed of 60,000 rpm and temperature of 298 K. The distributions of sedimentation coefficient $c(s_{20,w})$ and frictional ratio f/f_0 were computed using the SEDFIT software (version 15.01 c) (Schuck, 2000). The sedimentation coefficient $s_{20,w}$ was normalized to fit the value at 293 K in pure water. The weight fraction of each component was obtained from the corresponding peak area of $c(s_{20,w})$. The molecular weights were calculated from the corresponding peak positions $s_{20,w}$ and the frictional ratio f/f_0^2 (Brown and Schuck, 2006).

4.10 | SAXS measurements

SAXS and SEC-SAXS measurements were performed using NANOPIX (Rigaku, Japan) at 298 K. X-rays from a high-brilliance point-focused generator (MicroMAX-007 HFMR) were focused with a confocal multilayer mirror and two pinhole collimation system equipped with a lower parasitic scattering that provided x-rays at a flux of 2.0×10^8 cps at the sample position. The scattered x-rays were detected using a two-dimensional semiconductor detector (HyPix-6000) consisting of 765 × 813 pixels with a spatial resolution of 100 μm. The Q-range covered from 0.010 to 0.20 $Å^{-1}$ at the sample to the detector distance of 1330 mm. The detected two-dimensional scattering patterns were then converted to a one-dimensional scattering profile using circular averaging. After correction using the transmittance and subtraction of buffer scattering, the absolute scattering intensity was obtained using the standard scattering intensity of pure water at 298 K (1.632×10^{-2} cm^{-1}). All the above-described data reduction were conducted with the *SAngler* software (Shimizu et al., 2016). An ab initio model was built with a dummy atom method, DAMMIF in the ATSAS software package (version 3.1.3) based on the SAXS profile (Franke and Svergun, 2009). 7K7U.pdb and 1OKI.pdb were used to generate SAXS profiles for comparing with the experimental results in this study.

4.11 | SEC-SAXS measurements

SEC-SAXS measurements were performed using SEC–SAXS system (La-SSS) (Inoue et al., 2019). A Superdex™ 200 Increase 10/300 GL (Cytiva, USA) was used as the SEC column. To minimize the scattering from aggregates, the SEC column was first washed at a flow rate of 0.5 mL/min for 20 min. Then, the SEC-SAXS measurements were commenced after changing the flow rate to 0.02 mL/min.

4.12 | AUC-SAXS treatment

To eliminate the scattering caused by aggregates (or degradants) from the SAXS profile of the W59F tetramer solution, an AUC-SAXS treatment was applied to the SAXS profile (Morishima et al., 2020; Morishima et al., 2023).

AUTHOR CONTRIBUTIONS

Jiayue Sun: Writing – original draft; validation; funding acquisition. **Ken Morishima:** Investigation; data curation; validation. **Rintaro Inoue:** Investigation; validation. **Masaaki Sugiyama:** Writing – review and editing; resources. **Takumi Takata:** Writing – review and editing; funding acquisition; resources; project administration.

ACKNOWLEDGMENTS

The authors would like to thank Y. Kagasawa and N. Fujii for their technical support during the experiments. This work was supported by Japan Society for the Promotion of Science (grant number 23K10868). This work was also supported by Japan Science and Technology Agency (grant number JPMJFR2007), and the establishment of university fellowships toward the creation of science technology innovation (grant number JPMJFS2123).

ORCID

Takumi Takata https://orcid.org/0000-0003-3208-3704

REFERENCES

Andley UP. Crystallins in the eye: function and pathology. Prog Retin Eye Res. 2007;26:78–98.

Bax B, Lapatto R, Nalini V, Driessen H, Lindley PF, Mahadevan D, et al. X-ray analysis of beta B2-crystallin and evolution of oligomeric lens proteins. Nature. 1990;347:776–80.

Benedek GB. Cataract as a protein condensation disease: the Proctor Lecture. Invest Ophthalmol Vis Sci. 1997;38:1911–21.

Bloemendal H, de Jong W, Jaenicke R, Lubsen NH, Slingsby C, Tardieu A. Ageing and vision: structure, stability and function of lens crystallins. Prog Biophys Mol Biol. 2004;86:407–85.

Brown PH, Schuck P. Macromolecular size-and-shape distributions by sedimentation velocity analytical ultracentrifugation. Biophys J. 2006;90:4651–61.

Chaudhuri TK, Paul S. Protein-misfolding diseases and chaperone-based therapeutic approaches. FEBS J. 2006;273:1331–49.

Chen J, Callis PR, King J. Mechanism of the very efficient quenching of tryptophan fluorescence in human γD- and γS-crystallins: the γ-crystallin fold may have evolved to protect tryptophan residues from ultraviolet photodamage. Biochemistry. 2009;48:3708–16.

Chen J, Flaugh SL, Callis PR, King J. Mechanism of the highly efficient quenching of tryptophan fluorescence in human γD-crystallin. Biochemistry. 2006;45:11552–63.

Chiti F, Dobson CM. Protein misfolding, functional amyloid, and human disease. Annu Rev Biochem. 2006;75:333–66.

Ciechanover A, Kwon YT. Degradation of misfolded proteins in neurodegenerative diseases: therapeutic targets and strategies. Exp Mol Med. 2015;47:e147.

Das P, King JA, Zhou R. β-strand interactions at the domain interface critical for the stability of human lens γD-crystallin. Protein Sci. 2010;19:131–40.

Das P, King JA, Zhou R. Aggregation of γ-crystallins associated with human cataracts via domain swapping at the C-terminal β-strands. Proc Natl Acad Sci USA. 2011;108:10514–9.

Feng J, Smith DL, Smith JB. Human lens beta-crystallin solubility. J Biol Chem. 2000;275:11585–90.

Flaugh SL, Kosinski-Collins MS, King J. Contributions of hydrophobic domain interface interactions to the folding and stability of human γD-crystallin. Protein Sci. 2005;14:569–81.

Franke D, Svergun DI. DAMMIF, a program for rapid ab-initio shape determination in small-angle scattering. J Appl Crystallogr. 2009;42:342–6.

Fu L, Liang JJN. Unfolding of human lens recombinant βB2- and γC-crystallins. J Struct Biol. 2002;139:191–8.

Gillespie RL, O'Sullivan J, Ashworth J, Bhaskar S, Williams S, Biswas S, et al. Personalized diagnosis and management of congenital cataract by next-generation sequencing. Ophthalmology. 2014;121(2124–2137):e2121–2.

Hains PG, Truscott RJ. Proteomic analysis of the oxidation of cysteine residues in human age-related nuclear cataract lenses. Biochim Biophys Acta. 2008;1784:1959–64.

Harding JJ, Dilley KJ. Structural proteins of the mammalian lens: a review with emphasis on changes in development, aging and cataract. Exp Eye Res. 1976;22:1–73.

Inoue R, Nakagawa T, Morishima K, Sato N, Okuda A, Urade R, et al. Newly developed laboratory-based size exclusion chromatography small-angle x-ray scattering system (La-SSS). Sci Rep. 2019;9:12610.

Kosinski-Collins MS, Flaugh SL, King J. Probing folding and fluorescence quenching in human γD crystallin Greek key domains using triple tryptophan mutant proteins. Protein Sci. 2004;13:2223–35.

Kosinski-Collins MS, King J. In vitro unfolding, refolding, and polymerization of human γD crystallin, a protein involved in cataract formation. Protein Sci. 2003;12:480–90.

Lampi KJ, Ma Z, Hanson SR, Azuma M, Shih M, Shearer TR, et al. Age-related changes in human lens crystallins identified by two-dimensional electrophoresis and mass spectrometry. Exp Eye Res. 1998;67:31–43.

Lampi KJ, Murray MR, Peterson MP, Eng BS, Yue E, Clark AR, et al. Differences in solution dynamics between lens β-crystallin homodimers and heterodimers probed by hydrogen-deuterium exchange and deamidation. Biochim Biophys Acta. 2016;1860:304–14.

Mahler B, Doddapaneni K, Kleckner I, Yuan C, Wistow G, Wu Z. Characterization of a transient unfolding intermediate in a core mutant of γS-crystallin. J Mol Biol. 2011;405:840–50.

Mills IA, Flaugh SL, Kosinski-Collins MS, King JA. Folding and stability of the isolated Greek key domains of the long-lived human lens proteins γD-crystallin and γS-crystallin. Protein Sci. 2007;16:2427–44.

Moreau KL, King J. Hydrophobic core mutations associated with cataract development in mice destabilize human γD-crystallin. J Biol Chem. 2009;284:33285–95.

Moreau KL, King JA. Protein misfolding and aggregation in cataract disease and prospects for prevention. Trends Mol Med. 2012;18:273–82.

Morishima K, Inoue R, Sugiyama M. Derivation of the small-angle scattering profile of a target biomacromolecule from a profile deteriorated by aggregates. AUC-SAS. J Appl Crystallogr. 2023;56:624–32.

Morishima K, Okuda A, Inoue R, Sato N, Miyamoto Y, Urade R, et al. Integral approach to biomacromolecular structure by analytical-ultracentrifugation and small-angle scattering. Commun Biol. 2020;3:294.

Pande A, Pande J, Asherie N, Lomakin A, Ogun O, King J, et al. Crystal cataracts: human genetic cataract caused by protein crystallization. Proc Natl Acad Sci USA. 2001;98:6116–20.

Robman L, Taylor H. External factors in the development of cataract. Eye. 2005;19:1074–82.

Sagar V, Wistow G. Acquired disorder and asymmetry in a domain-swapped model for γ-crystallin aggregation. J Mol Biol. 2022;434:167559.

Sakthivel M, Elanchezhian R, Thomas PA, Geraldine P. Alterations in lenticular proteins during ageing and selenite-induced cataractogenesis in Wistar rats. Mol Vis. 2010;16:445–53.

Schafheimer N, King J. Tryptophan cluster protects human D-crystallin from ultraviolet radiation-induced photoaggregation. Photochem Photobiol. 2013;89:1106–15.

Schuck P. Size-distribution analysis of macromolecules by sedimentation velocity ultracentrifugation and Lamm equation modeling. Biophys J. 2000;78:1606–19.

Serebryany E, King JA. Wild-type human γD-crystallin promotes aggregation of its oxidation-mimicking, misfolding-prone W42Q mutant. J Biol Chem. 2015;290:11491–503.

Serebryany E, Takata T, Erickson E, Schafheimer N, Wang Y, King JA. Aggregation of Trp > Glu point mutants of human γ-D crystallin provides a model for hereditary or UV-induced cataract. Protein Sci. 2016;25:1115–28.

Shiels A, Hejtmancik JF. Mutations and mechanisms in congenital and age-related cataracts. Exp Eye Res. 2017;156:95–102.

Shimizu N, Yatabe K, Nagatani Y, Saijyo S, Kosuge T, Igarashi N. Software development for analysis of small-angle x-ray scattering data. AIP Conf Proc. 2016;1741:050017.

Sliney DH. How light reaches the eye and its components. Int J Toxicol. 2002;21:501–9.

Slingsby C, Wistow GJ. Functions of crystallins in and out of lens: roles in elongated and post-mitotic cells. Prog Biophys Mol Biol. 2014;115:52–67.

Smilgies DM, Folta-Stogniew E. Molecular weight-gyration radius relation of globular proteins: a comparison of light scattering, small-angle x-ray scattering and structure-based data. J Appl Crystallogr. 2015;48:1604–6.

Smith MA, Bateman OA, Jaenicke R, Slingsby C. Mutation of interfaces in domain-swapped human βB2-crystallin. Protein Sci. 2007;16:615–25.

Truscott RJW. Age-related nuclear cataract—oxidation is the key. Exp Eye Res. 2005;80:709–25.

Van Montfort RL, Bateman OA, Lubsen NH, Slingsby C. Crystal structure of truncated human βB1-crystallin. Protein Sci. 2003; 12:2606–12.

Vendra VP, Agarwal G, Chandani S, Talla V, Srinivasan N, Balasubramanian D. Structural integrity of the Greek key motif in βγ-crystallins is vital for central eye lens transparency. PLoS One. 2013;8:e70336.

Wenk M, Herbst R, Hoeger D, Kretschmar M, Lubsen NH, Jaenicke R. Gamma S-crystallin of bovine and human eye lens: solution structure, stability and folding of the intact two-domain protein and its separate domains. Biophys Chem. 2000; 86:95–108.

Wride MA. Lens fibre cell differentiation and organelle loss: many paths lead to clarity. Philos Trans R Soc Lond Ser B Biol Sci. 2011;366:1219–33.

Xi Z, Whitley MJ, Gronenborn AM. Human βB2-crystallin forms a face-en-face dimer in solution: an integrated NMR and SAXS study. Structure. 2017;25:496–505.

Xu J, Wang H, Wang A, Xu J, Fu C, Jia Z, et al. βB2 W151R mutant is prone to degradation, aggregation and exposes the hydrophobic side chains in the fourth Greek key motif. Biochim Biophys Acta Mol Basis Dis. 2021;1867:166018.

Yao K, Li J, Jin C, Wang W, Zhu Y, Shentu X, et al. Characterization of a novel mutation in the CRYBB2 gene associated with autosomal dominant congenital posterior subcapsular cataract in a Chinese family. Mol Vis. 2011;17:144–52.

Zhang K, Zhao WJ, Leng XY, Wang S, Yao K, Yan YB. The importance of the last strand at the C-terminus in βB2-crystallin stability and assembly. Biochim Biophys Acta Mol Basis Dis. 2014; 1842:44–55.

Zhao WJ, Xu J, Chen XJ, Liu HH, Yao K, Yan YB. Effects of cataract-causing mutations W59C and W151C on βB2-crystallin structure, stability and folding. Int J Biol Macromol. 2017;103: 764–70.

SUPPORTING INFORMATION

Additional supporting information can be found online in the Supporting Information section at the end of this article.

How to cite this article: Sun J, Morishima K, Inoue R, Sugiyama M, Takata T. Characterization of βB2-crystallin tryptophan mutants reveals two different folding states in solution. Protein Science. 2024;33(7):e5092. https://doi.org/10.1002/pro.5092